Research Journal of Applied Sciences, Engineering and Technology 10(3): 338-343, 2015
DOI: 10.19026/rjaset.10.2496
ISSN: 2040-7459; e-ISSN: 2040-7467

Submitted: December 29, 2014 Accepted: February 5, 2015 Published: May 30, 2015

Research Article

Design of Compact UWB Bandpass Filter with Improved Out-of-band Performance Using Distributed CRLH Transmission Lines

Gyuje Sung
Department of Electrical and Electronic Engineering and IITC, Hankyong National University,
327 Jungangro Ansung, Kyonggi-Do 456-749, Korea

Abstract: This study presents an Ultra-Wideband (UWB) filter with improved out-of-band performance. The proposed filter adopts novel Composite Right/Left-Handed (CRLH) Transmission Lines (TLs), which are modeled with distributed elements instead of lumped elements. A unit cell of the CRLH TLs is theoretically analyzed to derive the design formulas. The analyzing results confirm that the proposed structures are CRLH TLs. A novel UWB bandpass filter with improved out-of-band performance is designed and fabricated using the induced formulas. The measurement results show that the fabricated UWB bandpass filter has an insertion loss of less than 2.8 dB, a bandwidth of 2.8-10.4 GHz and a rejection of more than 18 dB from 11.6 to 23.4 GHz.

Keywords: Bandpass Filter (BPF), Composite Right/Left-Handed (CRLH) transmission line, group delay, Ultra-Wideband (UWB)

INTRODUCTION

Since the Federal Communications Commission (FCC) released the frequency band of 3.1-10.6 GHz for Ultra-Wideband (UWB) communications in 2002, UWB systems with high data rate, short-range and short-pulses have been rapidly developed for commercial purposes. Bandpass Filters (BPFs) are essential components of the UWB systems and thus have been studied extensively. Most of the UWB BPFs suffer from narrow upper stopbands and large overall sizes. Numerous filters have been designed using Multiple-Mode Resonators (MMRs) for improving upper-stopband performance. Some of these filters employed MMRs with lowpass structures structures (Wong *el al*., 2006; Wong and Zhu, 2007) and stub loaded MMRs, which are operated in quintuple or quadruple modes (Wong and Zhu, 2009; Deng *et al*., 2010; Wu *et al*., 2011). A Coplanar Waveguide (CPW) UWB BPF was proposed using MMR with stepped-impedance stubs (Honarvar and Sadeghzadeh, 2012). A radial stub loaded resonator with cross-shaped coupled lines was used to improve the out-of-band performance (Mohammadi *et al*., 2013). Defected Ground Structures (DGSs) were added to stub loaded or stepped-impedance stub loaded resonators (Yang *et al*., 2008; Tian and Chu, 2011; Gao *et al*., 2012). Moreover, UWB BPFs with improved out-of-band performance have been implemented using DGSs with a highpass filter or a BPF (Yang *et al*., 2007; Tang *et al*., 2008), BPFs with band stop filters (Li *et al*., 2008) and Composite Right/Left-Handed (CRLH) Transmission Lines (TLs) (Gong and Chu, 2008; Ahmed and Virdee, 2013). CRLH TLs can reduce the size and enhance the bandwidth of BPFs (Lai *et al*., 2004).

In this study, we present the design of a compact UWB BPF with improved out-of-band performance using novel distributed CRLH TLs. The dispersion characteristics of the distributed CRLH TLs are theoretically proved using even/odd-mode analysis method. The simulated and measured results of the proposed UWB BPF are in good agreement.

MATERIALS AND METHODS

The distributed CRLH TL unit cell shown in Fig. 1 is modeled with distributed elements instead of lumped elements. It cannot show explicitly which elements make Right-Handed (RH) TLs or Left-Handed (LH) TLs. The π equivalent circuit of the distributed CRLH TL unit cell can explain that the proposed unit cell is the CRLH TL unit cell. Because the circuit model is symmetrical, even/odd-mode analysis can be used to derive the π equivalent circuit and the transfer function. The even/odd-mode admittances of the unit cell of the distributed CRLH TLs are as follows:

$$Y_{even} = j\left(Y_2 \frac{Y_2 tan\theta_2 + Y_3 tan\theta_3 + Y_4 tan(\theta_4/2) + Y_5 tan(\theta_5/2)}{Y_2 - (Y_3 tan\theta_3 + Y_4 tan(\theta_4/2) + Y_5 tan(\theta_5/2)) tan\theta_2} - \frac{Y_1}{tan\theta_1}\right) \quad (1)$$

$$Y_{odd} = j\left(Y_2 \frac{Y_2 tan\theta_2 + Y_3 tan\theta_3 - Y_4 cot(\theta_4/2) - Y_5 cot(\theta_5/2)}{Y_2 - (Y_3 tan\theta_3 - Y_4 cot(\theta_4/2) - Y_5 cot(\theta_5/2)) tan\theta_2} - \frac{Y_1}{tan\theta_1}\right) \quad (2)$$

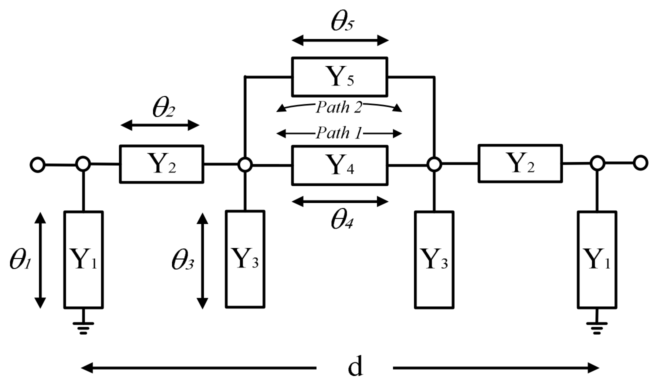

Fig. 1: Circuit model of the distributed CRLH TL unit cell

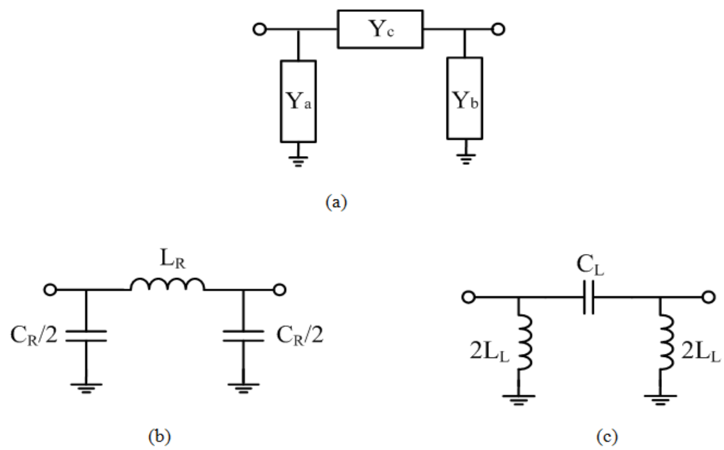

Fig. 2: (a) The π equivalent circuit of the distributed CRLH TL unit cell, (b) the π equivalent circuit when Y_a>0 and Y_c<0, (c) the π equivalent circuit when Y_a<0 and Y_c>0

The series and shunt branch elements of the π equivalent circuit in Fig. 2a are as follows:

$$Y_a = Y_b = Y_{even} \tag{3}$$

$$Y_c = \frac{Y_{odd} - Y_{even}}{2} \tag{4}$$

If Y_a>0 and Y_c<0, the distributed CRLH TL unit cell operates as a RH TL, as shown in Fig. 2b. If Y_a<0 and Y_c>0, it operates as an LH TL, as shown in Fig. 2c. The transfer function, S_{21}, can be expressed as:

$$S_{21} = \frac{(Y_{odd} - Y_{even})Y_0}{(Y_{even} + Y_0)(Y_{odd} + Y_0)} \tag{5}$$

where, Y_0 is the admittance of the input/output port. A transmission zero is created when $S_{21} = 0$, i.e.:

$$Y_{even} = Y_{odd} \tag{6}$$

Therefore, a transmission zero is created when:

$$Y_5 = \frac{2(tan^2\theta_{4,rej} - 1)}{sec^2\theta_{4,rej}} Y_4 \tag{7}$$

where, $\theta_{4,rej}$ is the electrical length at the transmission zero frequency, ω_{rej}, given by:

$$\omega_{rej} = \frac{\theta_{4,rej}}{\theta_{4,0}} \omega_0 \tag{8}$$

which is the resonant frequency of the series branch of the π equivalent circuit of the distributed CRLH TL unit cell and $\theta_{4,0}$ is the electrical length at the center frequency of the filter, ω_0. If $\theta_5 = 2\theta_4 = 360°$, the signals through paths 1 and 2 of the distributed CRLH TL unit cell shown in Fig. 1 are out of phase and cancel out to create another transmission zero. By using Bloch-Floquet theory, the dispersion relation and characteristic impedance of the unit cell can be expressed as (Pozar, 2012):

$$\gamma(\omega) = \frac{1}{d} cosh^{-1}(A) \tag{9}$$

$$Z_B(\omega) = B/\sqrt{A^2 - 1} \tag{10}$$

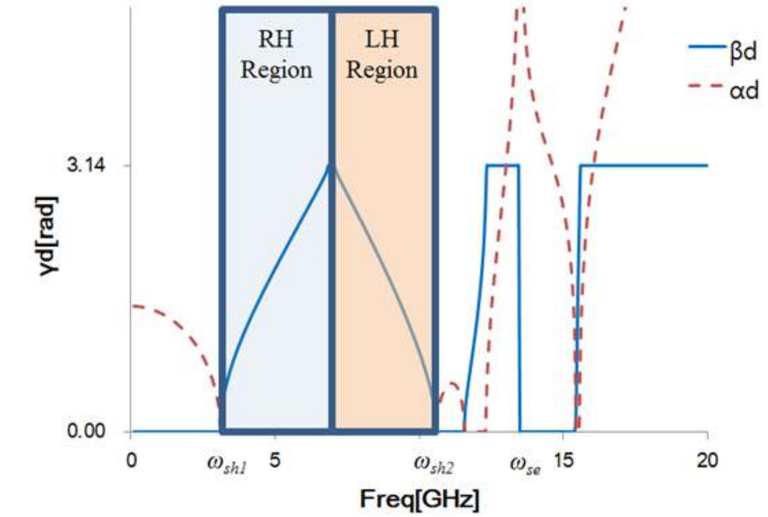

Fig. 3: Dispersion and attenuation diagram of the distributed CRLH TL unit cell

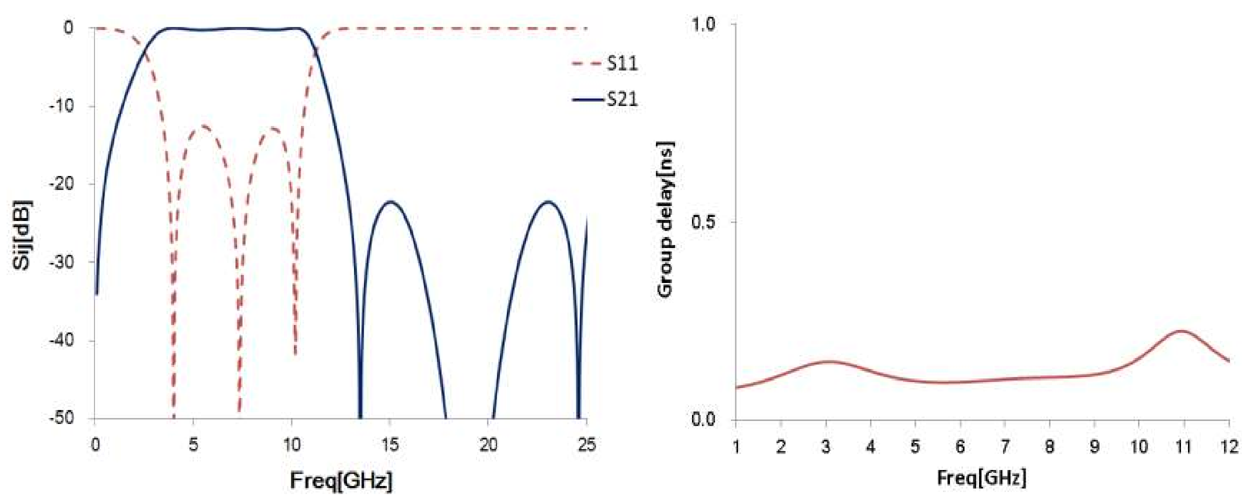

(a) (b)

Fig. 4: Frequency responses of the distributed CRLH TL unit cell, (a) amplitude, (b) group delay

where, Z_B is the characteristic impedance normalized to the port impedance, Z_0 and:

$$A = 1 + \frac{2Y_{even}}{Y_{odd-}Y_{even}} \tag{11}$$

$$B = \frac{2}{Y_{odd-}Y_{even}} \tag{12}$$

The dispersions and attenuations of the distributed CRLH TL unit cell are shown in Fig. 3, when $\theta_1 = \theta_4 = 60°$, $\theta_2 = \theta_3 = 30°$ and $\theta_5 = 120°$ at ω_0. The characteristic impedances of the stubs and TLs of the unit cell are determined using the method of the next paragraph. The calculated element values of the π equivalent circuit are as follows: from 3.1 to 7 GHz, Y_a>0 and Y_c<0 and from 7 to 10.6 GHz, Y_a<0 and Y_c>0. Therefore, in this distributed CRLH TL unit cell, the RH and LH regions are 3.1-7.0 and 7.0-10.6 GHz, respectively. At the resonant frequencies, ω_{shi}, of the shunt branch of Fig. 2a, γ = 0, thus indicating that the shunt branch is the parallel resonant circuit. The resonant frequency of the series branch is $\omega_{se} = \omega_{rej}$, namely, the series branch is the parallel resonant circuit. Therefore, the proposed unit cell is the CRLH TL unit cell. Figure 3 shows the wide passband characteristics between ω_{sh1} and ω_{sh2} and two attenuation poles at ω_{rej} and $3\omega_0$. Thus, the proposed distributed CRLH TL unit cell can be used to achieve wide out-of-band characteristics of a UWB BPF.

If the band edge frequencies, ω_{sh1} and ω_{sh2}, the transmission zero frequency, ω_{rej} and Z_B at ω_0 are given, we can calculate the characteristic impedances of each element of the unit cell using Eq. (5), (7), (9) and (10). One degree of freedom exists among the five characteristic impedances of the unit cell. Z_1 is a dominant parameter determining the slope parameter of the shunt resonator that creates the passband of the UWB BPF. Therefore, Z_1 is regarded as a free variable. The design specifications are as follows: the passband of the UWB BPF is 3.1-10.6 GHz, the attenuation pole frequencies are 13.5 and 19.0 GHz and the characteristic impedance of the distributed CRLH TL unit cell is 50 Ω at the center frequency. When Z_1 is set to 100 Ω, the calculated impedances are as follows: $Z_2 = 50$ Ω, $Z_3 = 86.1$ Ω, $Z_4 = 131.5$ Ω and $Z_5 = 107.9$ Ω. The frequency responses of the unit cell are shown in Fig. 4.

RESULTS AND DISCUSSION

The proposed UWB bandpass filter with improved out-of-band performance was implemented on a

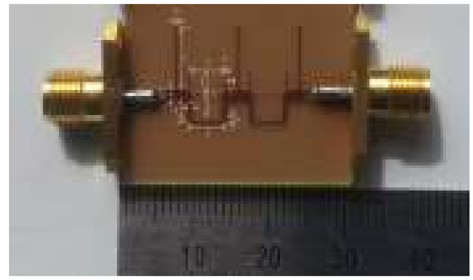

Fig. 5: Photograph of the fabricated UWB BPF

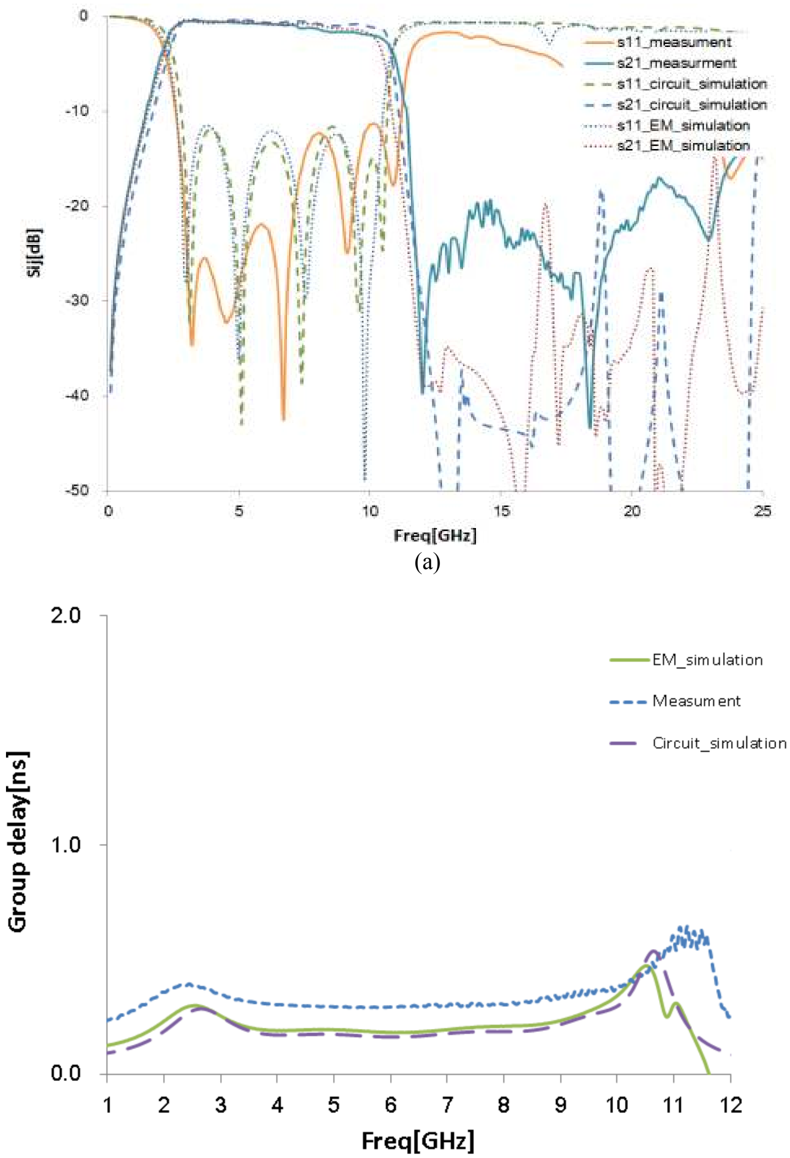

(a)

(b)

Fig. 6: Simulated and measured frequency responses of the UWB BPF, (a) wideband amplitude response, (b) group delay

Table 1: Comparison of UWB bandpass filters

Reference	Geo et al. (2012)	Tang et al. (2008)	Gong and Chu (2008)	Ahmed and Virdee (2013)	This study
Frequency (GHz)	3.07-10.69	3.10-10.60	3.0-10.6	2.90-10.75	2.80-10.40
Fractional bandwidth (%)	110	109	112	115	115
f_c (GHz)*	30.40	>19	19.1	16	23.40
Max. insertion loss (dB)	1.70	3.00	2.0	0.50	2.80
Min. return loss (dB)	10	15	13	11	11
Filter size (mm^2)	25.60×15.90	18.70×9.80	33×15	16.80×4.80	16.80×10.30
Max. group delay (nsec)	1.00	0.51	0.3	0.50	0.44

*: f_c is the maximum upper stopband frequency over an 18 dB rejection

0.6-mm thick FR-4 substrate with a dielectric constant of 4.4 and a loss tangent of less than 0.02. The fabricated UWB bandpass filter shown in Fig. 5 comprises two unit cells to ensure improved out-of-band performance. By using an Electromagnetic (EM) simulator, the dimensions of the structure were optimized to be as follows: w_1 = 1.17 mm, w_2 = 0.3 mm, w_3 = 0.55 mm, w_4 = 0.45 mm, w_5 = 0.2 mm, w_6 = 0.2 mm, l_1 = 6.5 mm, l_2 = 1.39 mm, l_3 = 2.35 mm, l_4 = 4.97 mm, l_5 = 2.48 mm, l_6 = 2.48 mm and l_7 = 4.57 mm. The size of the fabricated UWB BPF is 16.4×10.3 mm^2. The measurements were performed using an Anritsu 37347C vector network analyzer. Figure 6a shows the simulated and measured amplitude responses of the fabricated filter, which are in good agreement. The measured results show that the proposed UWB BPF has the insertion loss of less than 2.8 dB in the passband ranging from 2.8 to 10.4 GHz, the return loss over the passband is better than 11 dB and the rejection is more than 18 dB from 11.6 to 23.4 GHz. The simulated and measured group delays of the filter are drawn in Fig. 6b. The measured one varies between 0.29 and 0.44 nsec with a maximum variation of 0.15 nsec over the passband. The fabricated UWB BPF is more compact than those proposed by Gao *et al*. (2012) and Gong and Chu (2008) and has a simpler structure compared to Gao *et al*. (2012) and Tang *et al*. (2008), in which the UWB BPFs are implemented using DGSs. Its out-of-band performance is better than those of the previous works of Gong and Chu (2008) and Ahmed and Virdee (2013). The insertion losses of this study and Tang *et al*. (2008) are relatively large because they have been fabricated on FR-4 substrates, which have a relatively large loss tangent. Table 1 shows the performance comparison of this study and the previous works.

CONCLUSION

A UWB BPF with improved out-of-band performance that employs the distributed CRLH TLs is proposed in this study. The unit cell of the distributed CRLH TLs is theoretically analyzed to derive the dispersion characteristics and scattering parameters. The fabricated filter has a compact size, flat group delay and good out-of-band performance. The measured results are in good agreement with the simulation results.

ACKNOWLEDGMENT

This study was supported by the GRRC program of Gyeonggi province ((GRRC HANKYONG 2011-B01), Development of modular Transport System for cold storage warehouse).

REFERENCES

Ahmed, K.U. and B.S. Virdee, 2013. Ultra-wideband bandpass filter based on composite right/left handed transmission-line unit-cell. IEEE T. Microw. Theory, 61(2): 782-788.

Deng, H.W., Y.J. Zhao, X.S. Zhang, L. Zhang and S.P. Gao, 2010. Compact quintuple-mode UWB bandpass filter with good out-of-band rejection. Prog. Electromagn. Res. Lett., 14: 111-117.

Gao, M.J., L.S. Wu and J.F. Mao, 2012. Compact notched ultra-wideband bandpass filter with improved out-of-band performance using quasi electromagnetic bandgap structure. Prog. Electromagn. Res., 125: 137-150.

Gong, J.Q. and Q.X. Chu, 2008. SCRLH TL based UWB bandpass filter with widened upper stopband. J. Electromagnet. Wave., 22(14-15): 1985-1992.

Honarvar, M.A. and R.A. Sadeghzadeh, 2012. Design of coplanar waveguide ultrawideband bandpass filter using stub-loaded resonator with notched band. Microw. Opt. Techn. Let., 54(9): 2056-2061.

Lai, A., T. Itoh and C. Caloz, 2004. Composite right/left-handed transmission line metamaterials. IEEE Microw. Mag., 5(3): 34-50.

Li, Z., G.M. Wang, C.X. Zhang and G.N. Long, 2008. An ultra-wide bandpass filter with good out-of-band performance. Microw. Opt. Techn. Let., 50(7): 1735-1737.

Mohammadi, B., J. Nourinia, C. Ghobadi and A. Valizade, 2013. Design of compact UWB Band Pass filter using radial stub loaded resonator and cross-shaped coupled lines with improved out-of-band performance and sharp roll-off. Proceeding of Iranian Conference on Electrical Engineering (ICEE, 2013), pp: 1-5.

Pozar, D.M., 2012. Microwave Engineering. 4th Edn., Wiley, NJ.

Tang, I., D.B. Lin, C.M. Li and M.Y. Chiu, 2008. Ultra-wideband bandpass filter using hybrid microstrip-defected-ground structure. Microw. Opt. Techn. Let., 50(12): 3085-3089.

Tian, X.K. and Q.X. Chu, 2011. A compact UWB bandpass filter with improved out-of-band performance using modified coupling structure. Prog. Electromagn. Res. Lett., 22: 191-197.

Wong, S.W. and L. Zhu, 2007. EBG-embedded multiple-mode resonator for UWB bandpass filter with improved upper-stopband performance. IEEE Microw. Wirel. Co., 17(6): 421-423.

Wong, S.W. and L. Zhu, 2009. Quadruple-mode UWB bandpass filter with improved out-of-band rejection. IEEE Microw. Wirel. Co., 19(3): 152-154.

Wong, S.W., S. Sun, L. Zhu and Z.N. Chen, 2006. Ultra-wideband (UWB) bandpass filters with improved upper-stopband performance. Proceeding of Asia-Pacific Microwave Conference, pp: 29-32.

Wu, X.H., Q.X. Chu, X.K. Tian and X. Ouyang, 2011. Quintuple-mode UWB bandpass filter with sharp roll-off and super-wide upper stopband. IEEE Microw. Wirel. Co., 21(12): 661-663.

Yang, G.M., R. Jin, J. Geng, X. Huang and G. Xiao, 2007. Ultra-wideband bandpass filter with hybrid quasi-lumped elements and defected ground structure. IET Microw. Antenna. P., 1(3): 733-736.

Yang, G.M., R. Jin, C. Vittoria, V.G. Harris and N.X. Sun, 2008. Small ultra-wideband (UWB) bandpass filter with notched band. IEEE Microw. Wirel. Co., 18(3): 176-178.